Electronic Supplementary Material (ESI) for Inorganic Chemistry Frontiers.

SUPPORTING INFORMATION

Sequential Single-Crystal-to-Single-Crystal Vapochromic inclusion in non-porous coordination polymer: Unravelling dynamic rearrangement for selective pyridine sensing

Estefania Fernandez-Bartolome,[a] Esther Resines-Urien, [a] María Murillo-Vidal,[a] Lucía Piñeiro-Lopez*[a] and Jose Sanchez Costa*[a]

[a] IMDEA Nanociencia, C/ Faraday 9, Ciudad Universitaria de Cantoblanco, 28049, Madrid, Spain.

1)Experimental Section	**S1-S2**
2) Crystal Data for compounds 1, 2 and 3.	**S3**
3) Principal molecular interactions for compounds 1, 2 and 3	**S4-S5**
4) Selected distances and angles of the principal interactions	**S5-S7**
5) Powder X-ray Diffraction (PXRD) of compounds 1, 2 and 3	**S7**
6) FTIR Spectroscopy applied on compounds 1, 2 and 3	**S8**
7) Thermogravimetric analysis of compounds 1, 2 and 3	**S8-S9**
8) Reversibility of compound 3	**S10**
9) Reversibility of compound 3@PDMS	**S11**
10) BET analysis	**S11**
11) SCSC reaction set up	**S12**
12) 1@PDMS film profilometry	**S12-S13**
13) Crystal size change upon pyridine exposure	**S13**

1)Experimental Section

Materials. Chemicals and reagents were purchased from commercial suppliers and used as received.

Physical measurements.

- Crystal Structure Determination: The data were collected in a single crystal of **1**, **2** and **3** with a MD2M – Maatel diffractometer at the XALOC beamline (BL13) at ALBA Synchrotron with the collaboration of ALBA staff, from a Silicon (111) mono- chromator (T = 100 K, λ = 0.71073 Å).[1] The crystal was taken directly from its solution, mounted with a drop of Paratone-N oil and immediately put into the cold stream of dry N_2 on the goniometer. The structure was solved by direct methods and the refinement on F^2 and all further calculations were carried out with the SHELX-TL suite and OLEX2 program.[2]
- Optical reflectivity measurements were performed using a MOTIC SMZ-171 optical stereoscope coupled with a MOTICAM 3. Images were collected in BMP format without any filter using the Motic Images Plus 3.0 software, with the mean value from each region of interest (ROI) analyzed under the ImageJ program.
- TGA was performed using a TA Instrument TGAQ500 with a ramp of 1 ºC min^{-1} under air.
- FT-IR spectra were recorded as neat samples in the range 400-4000 cm^{-1} on a Bruker Tensor 27 (ATR device) Spectrometer.
- Elemental analyses (C, H, N) were performed on a LECO CHNS-932 Analyzer at the "Servicio Interdepartamental de Investigación (SIdI)" at Autónoma University of Madrid.
- Powder X ray diffraction data was collected in a Rigaku Smartlab SE diffractometer with a Bragg-Brentano configuration, using Cu-Kα radiation (λ = 0.1541 nm). The sample was measured between 5 and 50° with a speed of 1.8° min^{-1} under an X ray fluorescence reduction mode, at room temperature.
- Gas isotherms measurement was carried out on a Micromeritics Flowsorb 2300 at 77 K, with the temperature held constant using a liquid N_2 bath.
- Profilometry measurements were acquired with a DektakXT Bruker profilometer with a force of 1mg x g and with an acquisition time of 20 seconds.

Synthesis of $\{FeCl_2(pyrazine)_2\}_\infty$ (1)

A suspension of $FeCl_2 \cdot 4H_2O$ (81.12 mg, 0.408 mmol) and ascorbic acid (approx. 3 mg) in acetonitrile (2.5 mL) was added drop by drop to a suspension of pyrazine (96 mg, 1.19 mmol) in acetonitrile (2.5 mL) and the suspension was stirred for 15 minutes at room temperature. The resulting mixture was filtered and washed with acetonitrile, obtaining a red solid. Yield: 57 mg (31 %). Then, the red solid was dissolved in methanol at 50 °C. X-ray suitable red crystals of **1** were obtained by evaporation after 3 days.

FTIR (neat, cm^{-1}): 1667 (w), 1482 (w), 1411 (s), 1376 (m), 1154 (s), 1116 (s), 1087 (s), 1052 (s), 989 (w), 813 (s), 463 (s) (Figure 2a). Elemental analysis calculated (%) for $FeN_4C_8H_8Cl_2$. C 33.43, H 2.81 N 19.53; found C 33.70, H 2.58 N 19.75.

Synthesis of $\{FeCl_2(pyridine)_2(pyrazine)\}_\infty$ (2) and $[FeCl_2(pyridine)_4] \cdot H_2O$ (3)

Single crystals of **1** were put in a screw vial for chromatography (diameter 12 mm, height 32 mm). This tube was then placed in a clear glass simple vial (diameter 27 mm, height 55 mm) containing a saturated atmosphere of pyridine at room temperature. The vial was sealed to allow a gas phase/solid phase reaction between the pyridine and the crystals. After one day, orange crystals were obtained (intermediate product, **2**). If the complex **2** continues to be exposed to pyridine vapor, after 2 days the complete replacement of pyrazines occurs, obtaining the final compound (**3)**, yellow crystals. Both structures are suitable for X-ray diffraction analysis.

FTIR (neat, cm^{-1}) of compound **2**: 1652 (w), 1602 (w), 1482 (w), 1415 (s), 1164 (m), 1117 (s), 1053 (s), 813 (m), 789 (w), 755 (s), 693 (w), 632 (w), 406 (s), 414(w) (Figure 2a).

Elemental analysis calculated (%) for $FeN_4C_8H_8Cl_2$. C 46.06, H 3.87 N 15.35; found C 46.22, H 3.68 N 15.12.
FTIR (neat, cm^{-1}) of compound **3**: 1632 (w), 1597 (m), 1571 (w), 1484 (m), 1443 (s), 1246 (m), 1151 (m), 1073 (m), 1035 (s), 1006 (m), 984 (w), 944 (w), 878 (w), 755 (s), 694 (s), 621 (m), 420 (s) (Figure 2a). Elemental analysis calculated (%) for $FeN_4C_{20}H_{20}Cl_2.2H_2O$ C 50.13, H 5.05 N 11.69; found C 50.39, H 5.30 N 11.75.

Synthesis of (2') and (1') $\{FeCl_2(pyrazine)_2\}_\infty$
A pyrazine saturated $CHCl_3$ solution was placed in a glass vial provided with a plastic lid. Single crystals of **3** (70 mg) were added to the pyrazine solution and the vial was closed immediately. One day after, orange single crystals were filtered, washed with chloroform and allowed to dry giving rise to **2'** in 70% yield. **2'** was characterized by means of FTIR spectroscopy and XRPD measurements at room temperature. FTIR (neat, cm^{-1}) of compound **2'**: 1638 (m), 1600 (w), 1479 (w), 1411 (s), 1376 (m), 1213 (w), 1153 (s), 1141 (s), 1051 (s), 814 (s), 756 (s), 701 (m), 636 (w), 462 (s), 444 (s), 420 (m) (Figure S9).
When single crystals of **3** where left over 3 days in contact with the pyrazine saturated $CHCl_3$ solution, the red orange crystals (**2'**) underwent a colour change, first, from yellow to orange (**2'**) and then from orange to red, thus, single crystals of **1** (**1'**) were reobtained in a 40% yield. The product was characterized through FTIR spectroscopy and XRPD.
FTIR (neat, cm^{-1}) of compound **1'**: 1655 (m), 1638 (m), 1480 (w), 1410 (s), 1375 (m), 1152 (s), 1115 (s), 1050 (s), 987 (w), 812 (s), 460 (s), 443 (s), 417 (m) (Figure S9).

Synthesis of 1@PDMS, 3@PDMS and 1'@PDMS
1@PDMS film was prepared by mixing **1** powder (40mg) and 20 mg of dimethylvinyl-terminated dimethylsiloxane (PMDS)[39] to obtain a uniform mixture. Subsequently, the film was spin-coated on a Petri dish and placed in the oven at 70 °C for one hour. For the optical reflectivity measurements, a small square (50 x 50 mm) of **1@PDMS** was cut with a knife. The thickness of the **1@PDMS** composite varies between 57 μM and 60 μM, with the greatest thickness at the edge of the polymer (Figure S14 and S15).
FTIR (neat, cm^{-1}) of **1@PDMS**: 2962 (m), 2904 (w), 1638 (w), 1597 (m), 1484 (m), 1443 (m), 1412 (m), 1259 (s), 1215 (m), 1071 (s), 1016 (s), 864 (s), 843 (s), 794 (s), 755 (s), 694 (s), 621 (m), 601 (m), 462 (s) (Figure 4c).
1@PDMS was put in a screw vial for chromatography (diameter 12 mm, height 32 mm). Afterwards, this tube was placed in a clear glass simple vial (diameter 27 mm, height 55 mm) containing a saturated atmosphere of pyridine at room temperature. 6.5 hours after, a yellow film was obtained (**3@PDMS**).
FTIR (neat, cm^{-1}) of **3@PDMS**: 2962 (m), 2900 (w), 1663 (w), 1481 (w), 1448 (w), 1415 (m), 1257 (s), 1160 (m), 1066 (s), 1046 (s), 1013 (s), 861 (s), 844 (s), 792 (s), 756 (s), 692 (m), 601 (m), 509 (m), 460 (m) (Figure 4c).
When **3@PDMS** was immersed in an aqueous solution concentrated with pyrazine, the yellow film experienced an immediate colour change from yellow to red, **1'@PDMS**.
FTIR (neat, cm^{-1}) of **1'@PDMS**: 2962 (m), 2904 (w), 1638 (w), 1597 (m), 1484 (m), 1443 (m), 1411 (m), 1258 (s), 1049 (s), 1014 (s), 863 (s), 843 (s), 793 (s), 757 (s), 688 (s), 621 (m), 601 (m), 461 (s) (Figure S11).

2) Crystal Data for compounds 1, 2 and 3.

Table S1. Crystal data and structure refinement for compounds **1**, **2** and **3**.

Compound	(1)	(2)	(3)
CCDC	2035119	2035121	2035120
Chemical formula	$C_8H_8Cl_2FeN_4$	$C_{14}H_{14}Cl_2FeN_4$	$C_{20}H_{22}Cl_2FeN_4O$
Formula mass	286.93	365.04	461.16
Temperature (K)	100 K	100 K	100 K
Crystal system	Orthorhombic	Orthorhombic	Monoclinic
Space group	Ccce	Pbca	P1 21/n 1
***a*/Å**	10.212(2)	13.403(3)	9.38662(4)
***b*/Å**	10.527(2)	7.3710(15)	16.76565(6)
***c*/Å**	10.256(2)	15.995(3)	13.95424(6)
α/◦	90	90	90
β/◦	90	90	93.4342(4)
γ/◦	90	90	90
***V*(Å^3)**	1102.5(4)	1580.2(5)	2192.075(15)
Z	4	4	4
Radiation type	Synchrotron	Synchrotron	Synchrotron
Density (calculated g/cm^3)	1.729	1.534	1.397
Absorption coefficient (mm^{-1})	1.822	1.289	1.011
***F*(000)**	576	744	952
Crystal size (mm^3)	0.124 x 0.115 x 0.005	0.075 x 0.055 x 0.015	0.074 x 0.050 x 0.020
Goodness of fit on F^2	1.093	1.081	1.123
***R*1, *wR*2 [*I*>2σ(*I*)]**	0.0412, 0.1112	0.0404, 0.1137	0.0705, 0.2123
***R*1, *wR*2 (all data)**	0.0414, 0.1118	0.0410,0.1149	0.0722, 0.2163

3) Principal molecular interactions for compounds 1, 2 and 3.

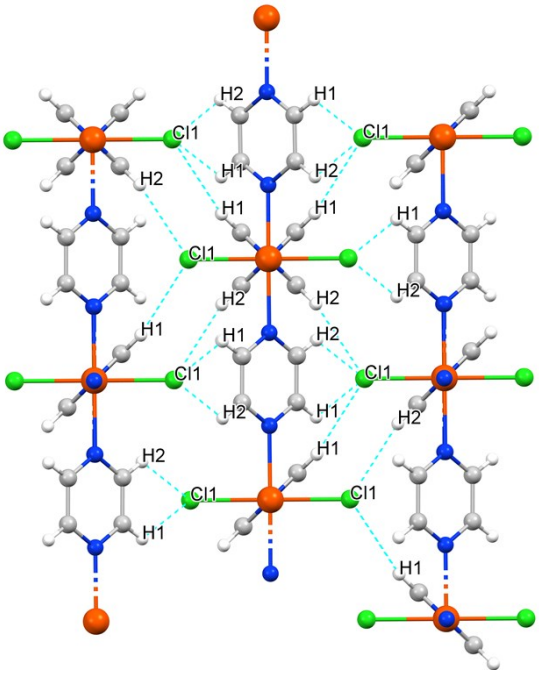

Figure S1. Principal supramolecular interactions in **1** between the chloride atoms in one layer and the hydrogens of the pyz rings of the adjacent layer along the b axis for **1.** The pyrazine rings in trans position are tilted 88.36° with respect to the Fe-N4 plane.

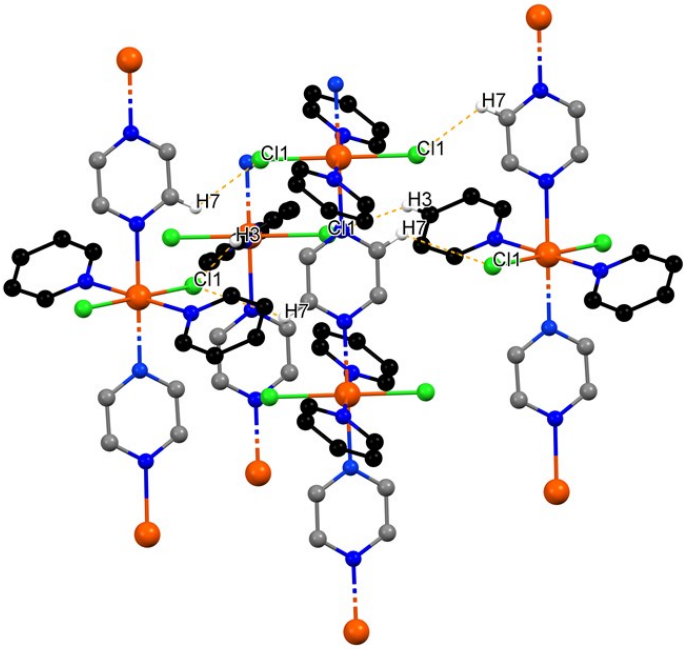

Figure S2. Principal supramolecular interactions between the chloride atoms in one layer and the hydrogens of the pz rings along the a axis, and the hydrogen atoms of the py with the chloride atoms along c axis of **2**.

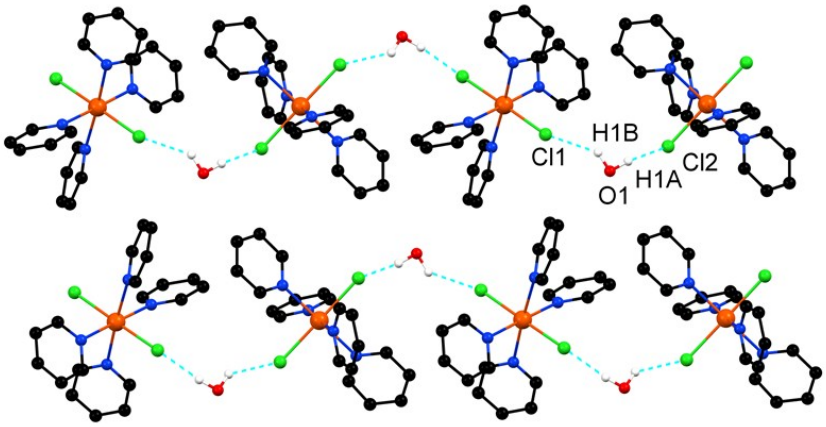

Figure S3. Principal hydrogen bonds in **3** between the chloride atoms in one layer and the hydrogens of the py rings along the ca axis of **3**. The pyridine rings in trans position are tilted 74.35° in opposite directions with respect to the N4-Fe-N2 and the N3-Fe-N1 axes, respectively.

4) Selected distances and angles of the principal interactions

Table S2. Selected bond lengths [Å] for compound **1**, **2** and **3**.

Compound	Bond	Distance (Å)	Supramolecular interaction	Distance (Å)	Supramolecular interaction	Distance (Å)
1	Fe1-N1(pz)	2.221	Cl1···C1-H1(pz)	3.555	Cl1···H1(pz)	2.930
	Fe1-Cl1	2.399	Cl1···C1-H2(pz)	3.555	Cl1···H2(pz)	2.924
2	Fe1-N1(py)	2.258	Cl1···C3-H3(py)	3.549	Cl1···H3(py)	2.762
	Fe1-N2(pz)	2.279	Cl1···C7-H7(pz)	3.581	Cl1···H7(pz)	2.947
	Fe1-Cl(1	2.395	Cl1···C6-H6(pz)	3.608	Cl1···H6(pz)	3.002
3	Fe1-N1(py)	2.251	Cl1···O1-H1B	3.145	Cl1···H1B	2.369
	Fe1-N2(py)	2.267	Cl2···O1-H1A	3.112	Cl2···H1A	2.236
	Fe1-N3(py)	2.242	Cl2···C17-H17(py)	3.618	Cl2···H17(py)	2.786
	Fe1-N4(py)	2.245	O1···C3-H3(py)	3.539	O1···H3(py)	2.707
	Fe1-Cl1	2.395	O1···C18-H18(py)	3.258	O1···H18(py)	2.406
	Fe1-	2.439				

	Cl2					

Table S3. Selected angles for compound **1**, **2** and **3**.

Compound	Atoms	Angle (°)
1	Cl1-Fe-N1(pz)	90.22
		89.78
	N1(pz)-Fe-N1(pz)	90.09
		89.91
2	Cl1-Fe-N1(py)	90.20
		89.80
	Cl1-Fe-N2(pz)	90.14
		89.86
	N1(py)-Fe-N2(pz)	95.63
		84.37
3	Cl1-Fe-N1(py)	91.48
	Cl1-Fe-N2(py)	90.33
	Cl1-Fe-N3(py)	90.51
	Cl1-Fe-N4(py)	89.81
	Cl2-Fe-N1(py)	90.79
	Cl2-Fe-N2(py)	90.94
	Cl2-Fe-N3(py)	87.29
	Cl2-Fe-N4(py)	88.96
	N1(py)-Fe-N2(py)	88.86
	N2(py)-Fe-N3(py)	88.26
	N3(py)-Fe-N4(py)	93.06
	N4(py)-Fe-N1(py)	89.81

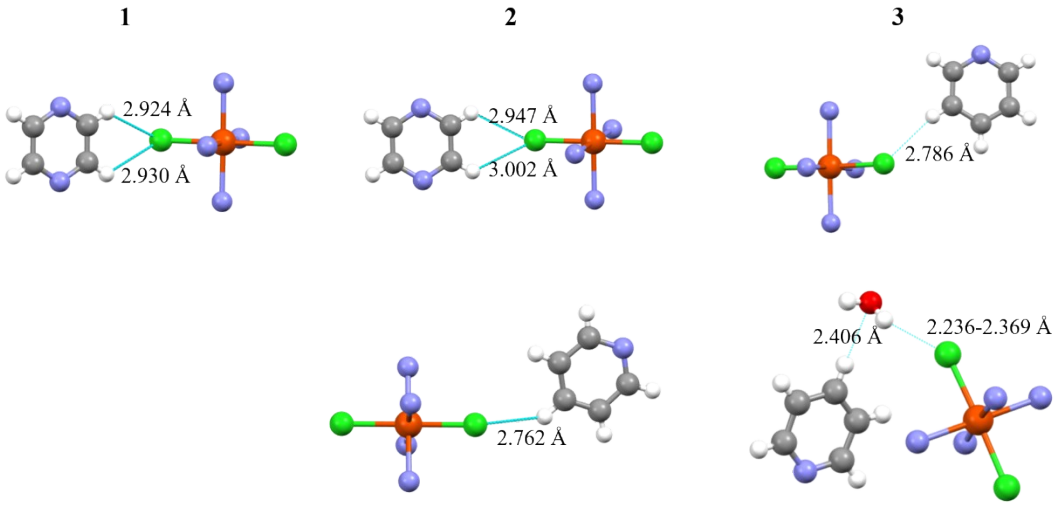

Figure S4. Principal supramolecular interactions in **1-3**.

5) Powder X-ray Diffraction (PXRD) of compounds 1, 2 and 3.

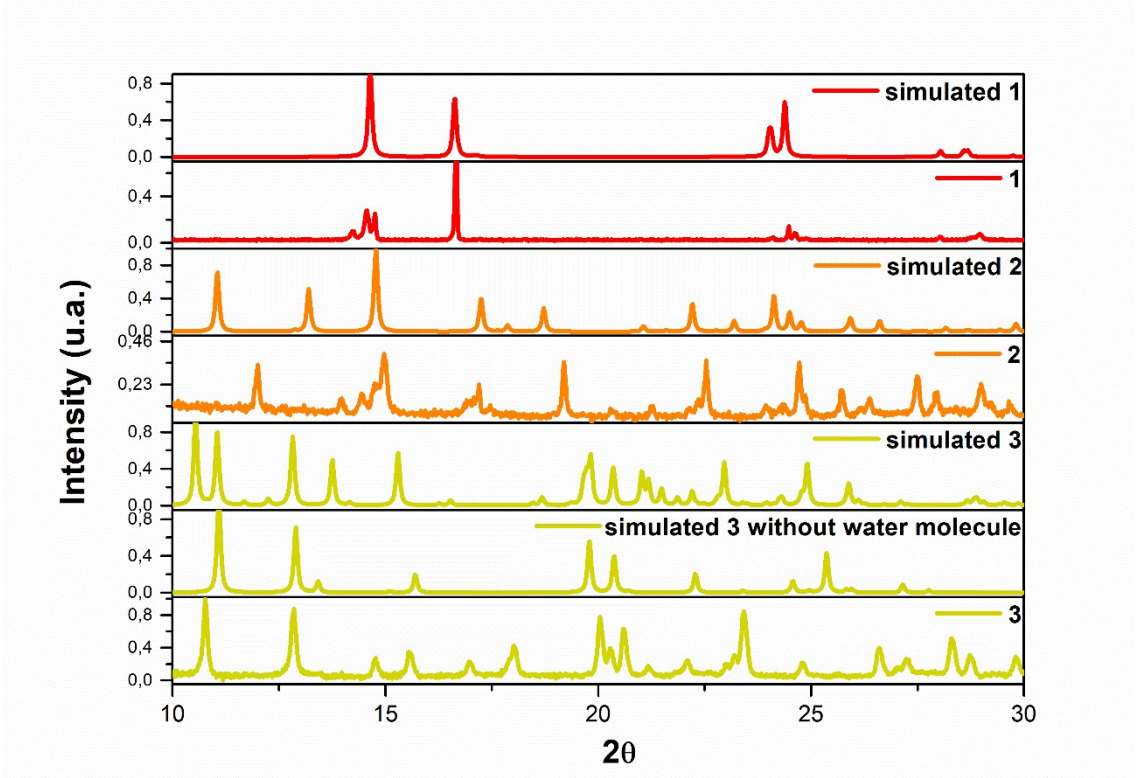

Figure S5. Simulated and experimental powder X-ray diffraction patterns of compounds **1, 2** and **3**.

6) FTIR spectroscopy applied on compounds 1, 2 and 3.

FTIR spectroscopy measurements applied on **1-3** confirmed the occurrence of the **1→2→3** SCSC gas/solid phase reaction.

Table S4. IR band assignment for compounds **1**, **2** and **3**.

Compound	IR band assignment	Wavelength interval (cm^{-1})
1	νring(pz)	1595-1440
	δC-H(pz)	1163-1056
	γring(pz)	463
2	νring (pz)	1411
	δC-H(pz)	1118-1056
	γring(pz)	463
	δC-H(pz)	1118-1056
	δC-H(py)	1154, 1011, 755, 619
	γring(py)	463
3	νring (py)	1595-1440
	δC-H(py)	1216-1003
	γring(py)	419

ν: stretching, δ: bending in-plane, γ: bending out of plane

7) Thermogravimetric analysis of compounds 1, 2 and 3

To provide an insight into the thermal stability of the compounds, thermogravimetric analyses were carried out for **1-3** (Figures S6-S8). **1** loses mass above 100 °C whereas **2** is stable only below 40 °C. In **3**, the weight loss of 3.9 % taking place above 50 °C, corresponds to the release of the water molecules observed by X-ray diffraction (Fe/H_2O 1:1).

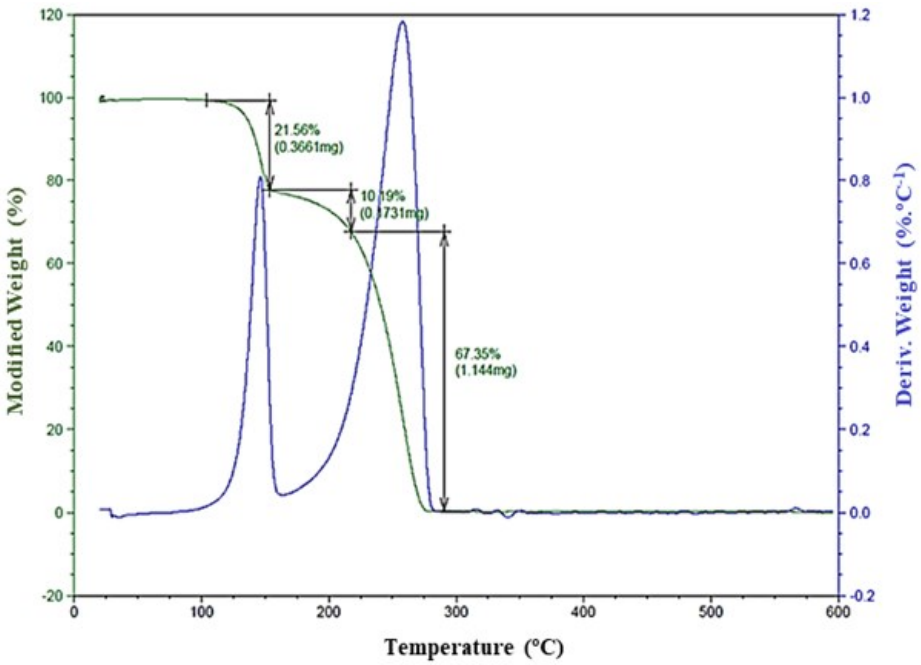

Figure S6. Thermogravimetric profile of **1** (1.2820 mg in air showing the mass variation (green curve) and its first derivative (blue curve) upon heating at 2 ºC/min.

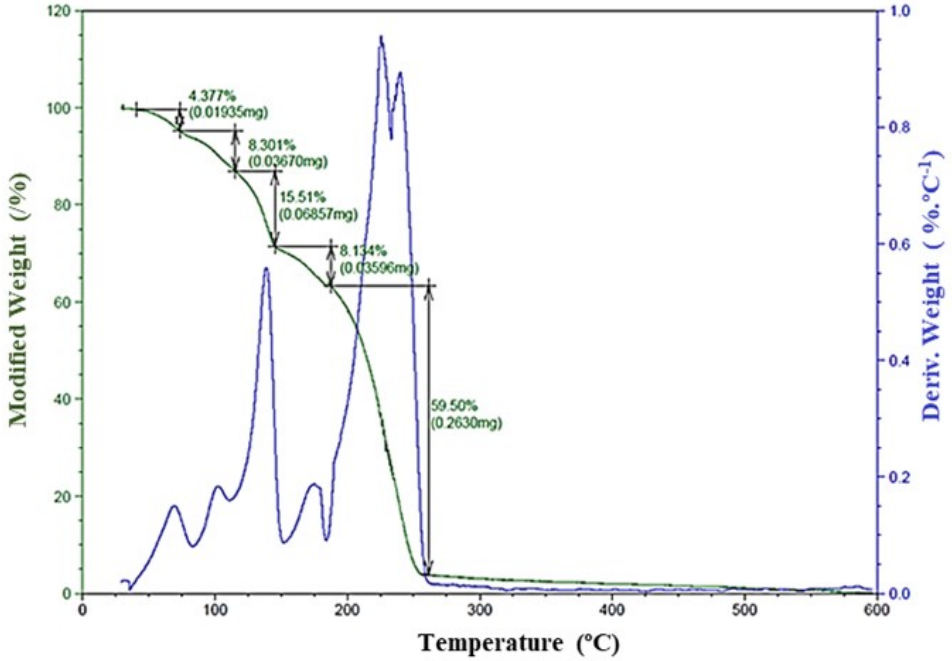

Figure S7. Thermogravimetric profile of **2** (0.6560 mg in air showing the mass variation (green curve) and its first derivative (blue curve) upon heating at 2 ºC/min.

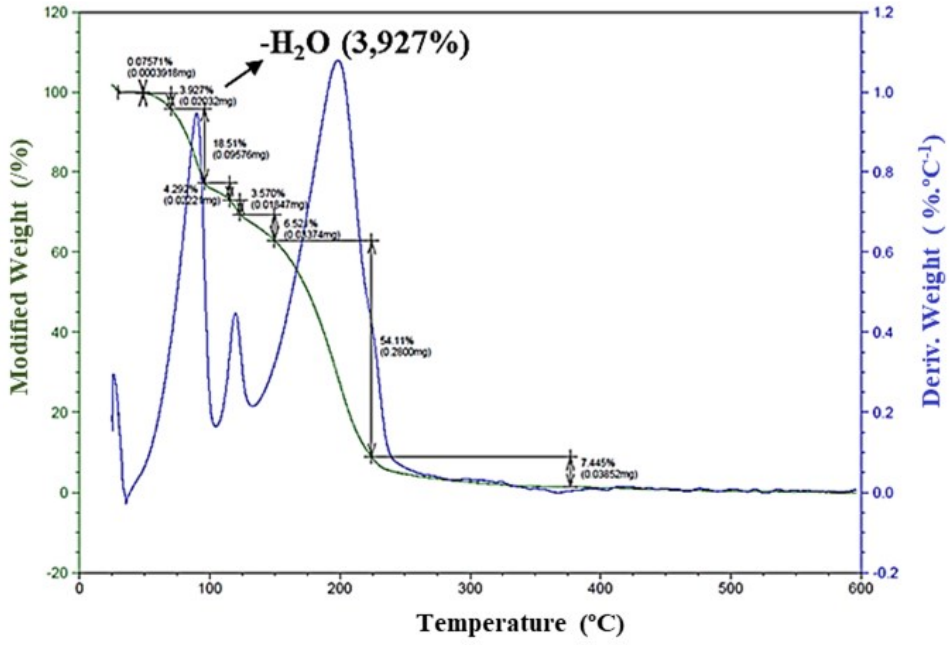

Figure S8. Thermogravimetric profile of **3** (0.8650 mg in air showing the mass variation (green curve) and its first derivative (blue curve) upon heating at 2 ºC/min.

8) Reversibility of compound 3

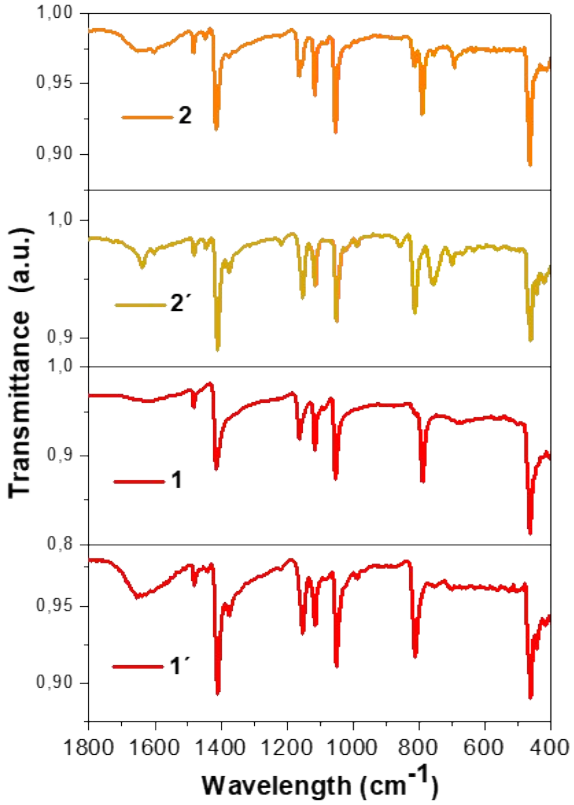

Figure S9. Infrared spectra of compounds **2**, **2'**, **1** and **1'**.

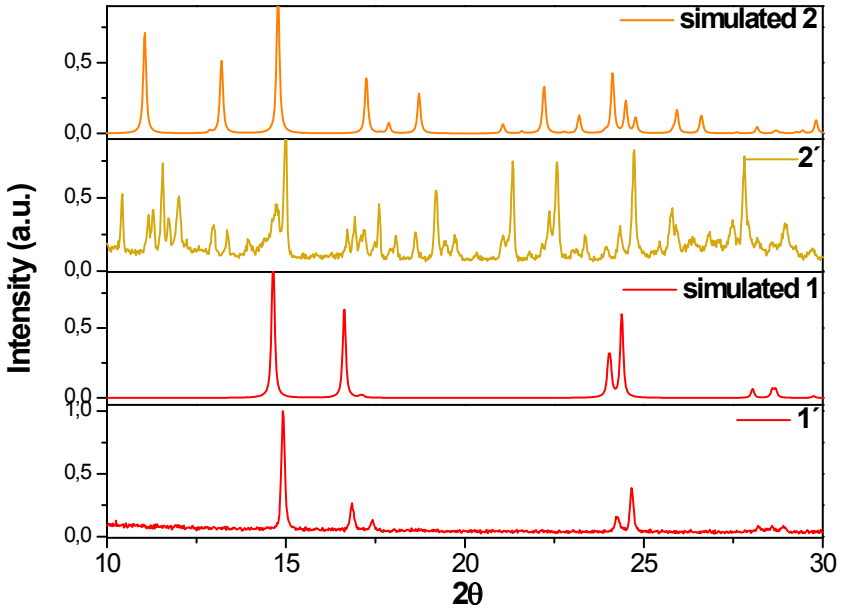

Figure S10. Simulated and experimental powder X-ray diffraction patterns of compounds **2**, **1** and **2'** and **1'**, respectively.

9) Reversibility of compound 3@PDMS

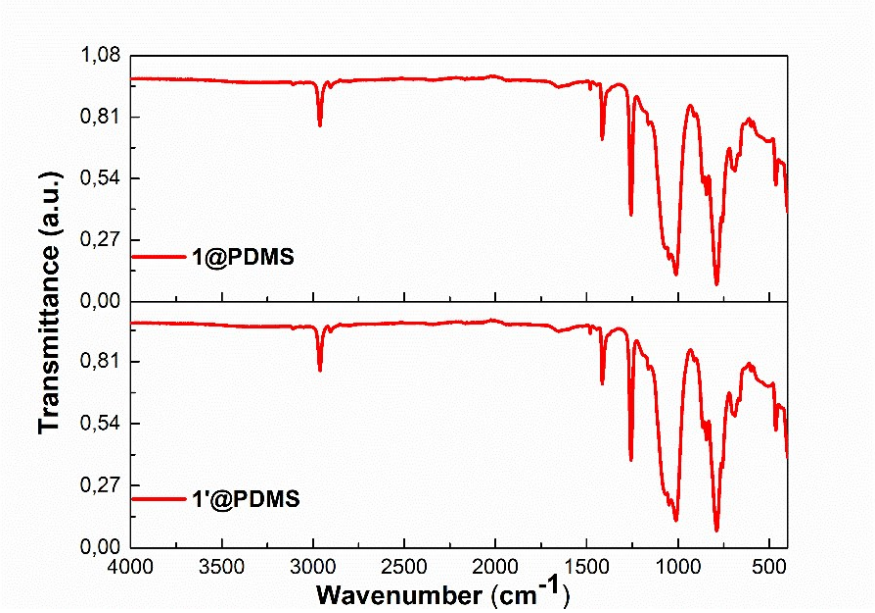

Figure S11. FTIR spectra of compounds **1@PDMS** and **1'@PDMS**.

10) BET Analysis

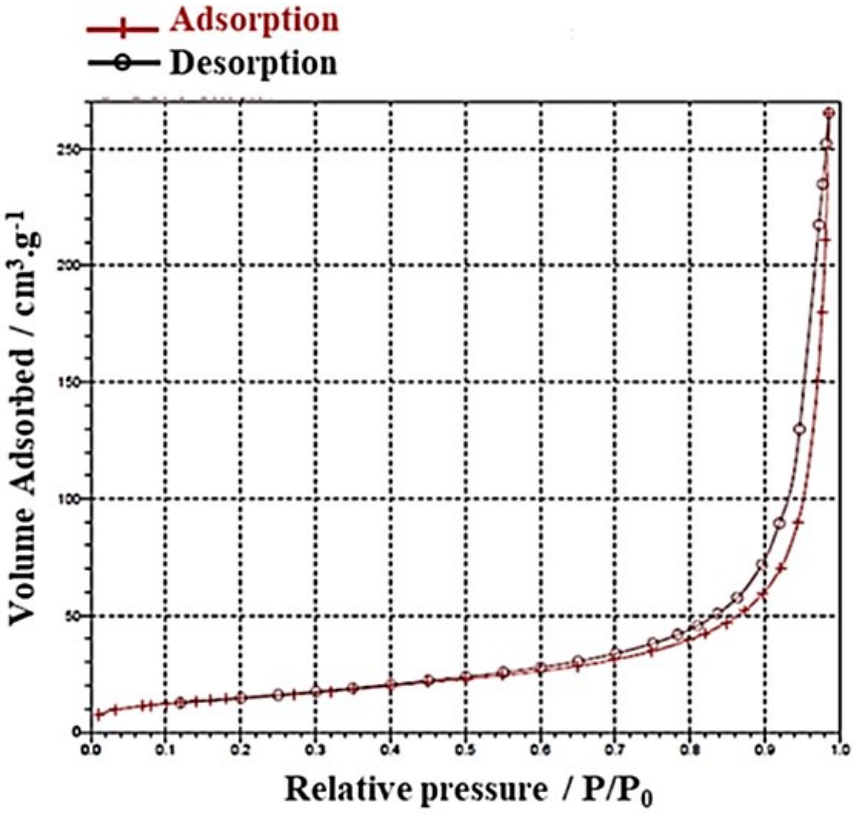

Figure S12. Nitrogen gas sorption isotherm at 78 K for compound **1** (open circles, adsorption; crosses, desorption). P/P_0 is the ratio of gas pressure (P) to saturation pressure (P_0), with P_0 being 716 torr.

11) SCSC reaction set up

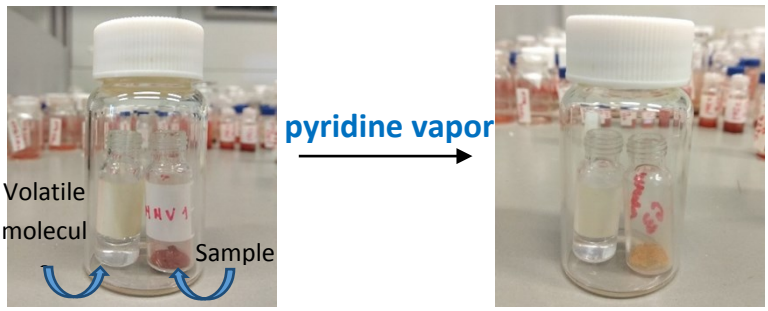

Figure S13. Illustration of the SCSC reaction set up described in this work.

12) 1@PDMS film profilometry

Figure S14. Profilometry for **1@PDMS** at the edge of the film.

Figure S15. Profilometry for **1@PDMS** at the center of the film.

13) Crystal size change upon pyridine exposure

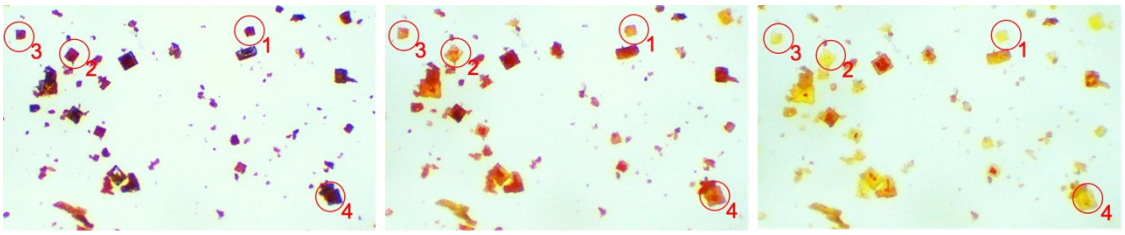

Crystal	$Distance_{red}$ (µm)		$Distance_{orange}$ (µm)		$Distance_{yellow}$ (µm)		$\Delta A_{red\text{-}orange}$ (%)	$\Delta A_{red\text{-}yellow}$ (%)
1	46,08	53,34	62,42	68,12	59,18	80,76	42,2	48,6
2	70,18	62,77	90,84	70,18	94,15	83,3	30,9	43,8
3	56,14	42,11	65,66	51,67	70,33	74,85	30,3	55,1
4	100,99	84,73	118,35	105,55	130,32	142,29	31,5	53,8
Mean	68,35	60,74	84,32	73,88	88,50	95,30	33,7	50,3

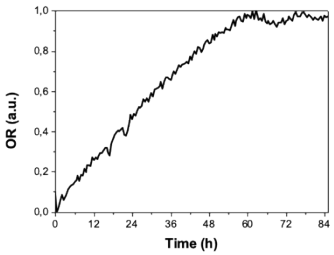

Figure S16. Colour and crystal size evolution as Single-Crystal-to-Single-Crystal transformation from **1→2→3** for four different crystals. Below on the right the optical reflectivity measured for crystal 1.